JOURNAL OF BACTERIOLOGY, Jan. 2007, p. 160–168 Vol. 189, No. 1
0021-9193/07/$08.00+0 doi:10.1128/JB.01425-06

Malic Enzyme Cofactor and Domain Requirements for Symbiotic N_2 Fixation by *Sinorhizobium meliloti*▽†

Michael J. Mitsch, Alison Cowie, and Turlough M. Finan*

Center for Environmental Genomics, Department of Biology, McMaster University, 1280 Main Street West, Hamilton, Ontario, Canada L8S 4K1

Received 7 September 2006/Accepted 17 October 2006

The NAD^+-dependent malic enzyme (DME) and the $NADP^+$-dependent malic enzyme (TME) of *Sinorhizobium meliloti* are representatives of a distinct class of malic enzymes that contain a 440-amino-acid N-terminal region homologous to other malic enzymes and a 330-amino-acid C-terminal region with similarity to phosphotransacetylase enzymes (PTA). We have shown previously that *dme* mutants of *S. meliloti* fail to fix N_2 (Fix^-) in alfalfa root nodules, whereas *tme* mutants are unimpaired in their N_2-fixing ability (Fix^+). Here we report that the amount of DME protein in bacteroids is 10 times greater than that of TME. We therefore investigated whether increased TME activity in nodules would allow TME to function in place of DME. The *tme* gene was placed under the control of the *dme* promoter, and despite elevated levels of TME within bacteroids, no symbiotic nitrogen fixation occurred in *dme* mutant strains. Conversely, expression of *dme* from the *tme* promoter resulted in a large reduction in DME activity and symbiotic N_2 fixation. Hence, TME cannot replace the symbiotic requirement for DME. In further experiments we investigated the DME PTA-like domain and showed that it is not required for N_2 fixation. Thus, expression of a DME C-terminal deletion derivative or the *Escherichia coli* NAD^+-dependent malic enzyme (*sfcA*), both of which lack the PTA-like region, restored wild-type N_2 fixation to a *dme* mutant. Our results have defined the symbiotic requirements for malic enzyme and raise the possibility that a constant high ratio of NADPH + H^+ to NADP in nitrogen-fixing bacteroids prevents TME from functioning in N_2-fixing bacteroids.

Members of the *Rhizobiaceae* enter into a symbiotic association with a plant host, during which time the free-living bacteria differentiate into nitrogen-fixing cells known as bacteroids. This transition is accompanied by a number of important physiological adaptations, among which are alterations to the metabolic pathways of the microbe (14). There is much evidence to suggest that bacteroids within nodules utilize C_4-dicarboxylic acids as their primary carbon and energy sources and that these acids are metabolized via the tricarboxylic acid (TCA) cycle (13, 30, 31, 43). A number of reports have suggested that cycling of amino acids between the plant and bacteroid also plays a key role in carbon and nitrogen flow in N_2-fixing root nodules (1, 24, 40). These reports have demonstrated that much remains to be resolved concerning C and N flow between the bacteroid and plant during symbiotic N_2 fixation.

In N_2-fixing bacteroids metabolizing C_4-dicarboxylic acids via the TCA cycle, a pathway for the generation of acetyl coenzyme A (acetyl-CoA) is essential. One route for the formation of acetyl-CoA is via malic enzyme and pyruvate dehydrogenase (7, 8). Malic enzymes are responsible for the conversion of malate to pyruvate with the concomitant reduction of a nicotinamide cofactor. *Sinorhizobium meliloti* contains two malic enzymes, DME (diphosphopyridine nucleotide-dependent malic enzyme), which is dependent on $NAD(P)^+$ (EC 1.1.1.39), and TME (triphosphopyridine nucleotide dependent malic enzyme), which utilizes $NADP^+$ exclusively (EC 1.1.1.40) (39). *S. meliloti dme* mutants were shown to form root nodules which fail to fix nitrogen (7), while *tme* mutants formed wild-type nitrogen-fixing root nodules (7, 8). Biochemical characterization of DME and TME revealed that the enzymes have similar kinetic parameters and have almost identical K_ms for substrate and cofactor, indicating that the enzymes should have similar rates of activity (39). The enzymes do differ in their responses to TCA cycle intermediates, with DME activity being enhanced by fumarate, succinate, and malate but inhibited by acetyl-CoA (9, 39).

Here we employed specific antibodies to directly quantify the levels of malic enzymes in free-living cells and bacteroids, and we found that TME protein levels in bacteroids are 20% of those in free-living cells. These data suggested that the reduced levels of TME in bacteroids could be the reason for its failure to functionally replace DME in *dme* mutant strains. We investigated this question by determining the symbiotic phenotypes of *dme* mutant strains carrying chromosomally integrated constructs in which (i) *tme* is expressed from the *dme* promoter and (ii) *dme* is expressed from the *tme* promoter.

The analysis of the symbiotic requirement for malic enzymes is complicated by the unusual bipartite structure of the DME and TME enzymes of *S. meliloti*. DME and TME are 770 and 761 amino acids in length, respectively, and are members of a large family of malic enzymes that contain an approximately 300-amino-acid domain at their C termini that is not present in other prokaryotic and eukaryotic malic enzymes, such as the 478- and 389-amino-acid enzymes from *Bacillus stearothermophilus* (19) and *Streptococcus bovis* (18), respectively (26).

* Corresponding author. Mailing address: McMaster University, Department of Biology, 1280 Main St. West, Hamilton L8S 4K1, Canada. Phone: (905) 525-9140, ext. 24400. Fax: (905) 522-6066. E-mail: finan@mcmaster.ca.

† Supplemental material for this article may be found at http://jb.asm.org/.

▽ Published ahead of print on 27 October 2006.

The C-terminal extension shows similarity to phosphotransacetylase enzymes (PTA) (EC 2.3.1.8) that are responsible for the interconversion of acetyl-CoA and acetyl phosphate. The widespread prevalence of the PTA-like domain suggests functional relevance; however, deletion of the C-terminal region of the *S. meliloti* malic enzymes did not abolish malic enzyme activity (26). We wished to determine if the C-terminal extension is required during symbiosis. To accomplish this task, two experimental procedures were carried out. First, the NAD^+-dependent malic enzyme of *Escherichia coli*, SfcA (36), a protein that lacks the PTA-like extension, was expressed from the *dme* promoter in *dme*-deficient *S. meliloti* strains. Second, a truncated form of DME that lacks the C-terminal domain but still retains malic enzyme activity (26) was expressed in *dme*-deficient *S. meliloti* strains. Both constructs were analyzed in plant and enzyme assays in order to determine if either construct was able to support symbiotic nitrogen fixation.

MATERIALS AND METHODS

Bacterial strains and genetic methods. *E. coli* cells were grown at 37°C in Luria-Bertani broth (LB), while *S. meliloti* cells were grown at 30°C in LBmc (LB supplemented with 2.5 mM $MgSO_4$ and 2.5 mM $CaCl_2$) and minimal medium (M9) with carbon sources at 15 mM as previously described (8). *E. coli* strain EJ1321 (*pck dme tme*) (16) and *S. meliloti* strain RmH194 (*pckA1*::Tn*3*HoHo *pod-1 dme-1*::Tn*5 tme-4*::ΩSp) (8) fail to grow on minimal medium with succinate as a carbon source. Complementation of this growth phenotype was used to determine whether the malic enzyme constructs created in this work were functional.

Derivatives of the gentamicin-resistant suicide vector pUCP30T (34) were mobilized into *S. meliloti* by triparental matings as previously described (11). Recombinants were selected on LBmc plates containing 20 μg/ml gentamicin (Gm) plus neomycin (Nm; 200 μg/ml), spectinomycin (Sp;100 μg/ml), or streptomycin (Sm; 200 μg/ml) as required. Because the pUCP30T chimeric malic enzyme constructs carried *S. meliloti* DNA from both the *tme* and *dme* gene regions, these constructs could recombine at either the *tme* or *dme* locus. To identify the cointegrate-recombination class, phage ΦM12 was used to transduce the Gm-resistant (Gm^r) marker of pUCP30T and either the *dme* or *tme* mutation antibiotic resistance marker from individual recombinants into the wild-type strain Rm1021 (10). Approximately 30 clones from each transduction were replica plated onto LBmc plates containing neomycin (for the *dme* Tn*5* mutations) or LBmc plates containing spectinomycin (for the *tme* ΩSp mutation) and gentamicin (the antibiotic marker for pUCP30T). Cotransduction of both the Gm^r and the *dme* or *tme* antibiotic resistance marker demonstrated linkage between pUCP30T and the demonstrated recombination at the particular locus of interest. In all cases, recombination at the targeted structural gene was achieved with the pUCP30T vector construct containing the same structural gene, and these strains were utilized for further experimentation. Crude cell extracts and bacteroid extracts were produced according to previous protocols (7, 12).

Molecular biology techniques and introduction of SphI sites into the *dme* and *tme* genes. General molecular biology methodologies were performed according to standard techniques. To facilitate manipulation of the *tme* and *dme* genes of *S. meliloti*, an SphI site was inserted at the previously identified translational start sites with the primers 5′-GATACCCGGCATGCTTCCTCAACCTC-3′ and 5′-CGCCCGTGTGCATGCCTTTGC-3′, respectively, following the procedure of Kunkel et al. (22). The templates used for site-directed mutagenesis were produced from truncated regions of *tme* and *dme*. For *dme*, pTH139 containing the entire *dme* open reading frame was digested with SalI and religated to yield plasmid pTH398, containing 868 bp of the *dme* open reading frame. For *tme*, pTH251 (26) was digested with *Bsp*HI, end filled with Klenow polymerase, and digested with EcoRI. The resulting 480-bp fragment was gel purified and ligated into pUC119 digested with SphI, treated with Klenow polymerase, and redigested with EcoRI to produce pTH399. These plasmids were then transformed into *E. coli* strain CJ236 (*ung dut*) to generate single-stranded DNA (22). The resulting plasmids were transformed into DH5α cells and then screened for the presence of an SphI site. On average, 50% of the transformants contained the desired mutation. Following DNA sequencing to verify sequence integrity, the *dme* and *tme* constructs pTH400 and pTH401B, respectively, were used in further experiments. The full-length genes were reconstituted such that both genes would retain the SphI at the translational start site. *dme* was reconstructed by inserting the SalI fragment from pTH139 into pTH400 to produce pTH408. *tme* was reconstructed by inserting a 2.5-kb EcoRI fragment from pTH392 into pTH401B, resulting in pTH407B.

Production of the p*dme-tme* construct. To introduce *tme* downstream of the *dme* promoter, pTH408 was digested with SphI and KpnI, and the resulting 3.8-kb vector-*dme* promoter fragment was gel purified. Digesting pTH407B with SphI and KpnI and gel purifying the resulting 2.7-kb fragment isolated the *tme* structural gene. The two fragments were ligated to generate the plasmid pTH409. Transformants of *E. coli* EJ1321 carrying pTH409 grew on M9 minimal medium with succinate as the sole carbon source, verifying that pTH409 produced a functional TME product. To introduce the hybrid construct into *S. meliloti*, the 3.5-kb p*dme-tme* fragment was isolated with HindIII and KpnI and inserted into the similarly digested vector pUCP30T, to give pTH433. This cloning strategy resulted in the p*dme-tme* construct being inserted in the orientation opposite that of the *lacZ* promoter present on this plasmid, thus removing the possibility that a promoter other than *dme* could be responsible for expressing *tme*. Cointegration of pTH433 at the *tme* gene loci was verified by transduction.

Production of the p*tme-dme* construct. pTH407B was digested with HindIII and EcoRI, producing a 487-bp *tme* fragment that was inserted into pBluescript KS. A 2.98-kb *dme* fragment from pTH408 was isolated following digestion with HindIII and inserted into a similarly digested pBluescript KS vector. This resulted in the *dme* structural gene being inserted in the vector such that the BamHI site was in the 3′ region of the gene. These two constructs allowed the use of the SphI site located in both fragments that were previously inserted into the translational start site of both genes. The final construct was produced by removing the 2.8-kb *dme* fragment via a SphI/BamHI digest followed by insertion downstream of the *tme* promoter in pBluescript KS, resulting in pTH596. This construct resulted in 471 bp of the *tme* promoter being positioned upstream of the *dme* open reading frame, with the translational start site of *dme* being fused to the translational start site of *tme* via the SphI site. The 3.3-kb hybrid construct was then digested with BamHI and KpnI and inserted into pUCP30T to create plasmid pTH597. A triparental mating was carried out to introduce the construct into various *dme*::Tn*5* mutant *S. meliloti* strains, and transductions were carried out to verify recombination at the *dme* gene loci as described above.

Production of p*dme-sfcA*. The *sfcA* gene was amplified from the plasmid pMEE1 (36) using the primers 5′-GAA ACA GA**G CAT GC**A ACC AAA AAC AAA AAA AC-3′ and 5′-CTC TCA TCC GCC AAA ACA GCC-3′ (bold type indicates the SphI restriction site introduced in the PCR fragment at the translational start site of *sfcA*). The resulting 1.8-kb fragment was digested with SphI and PstI and ligated to the plasmid pTH408, which was similarly digested. This ligation replaced the *dme* structural gene of pTH408 with the *sfcA* gene in such a way that *sfcA* was positioned downstream of the *dme* promoter. The resulting plasmid, pTH512, was digested with HindIII and PstI, and the 2.1-kb fragment (p*dme-sfcA*) was inserted into pUCP30T, also digested with HindIII and PstI, to generate pTH513. Plasmid pTH513 complemented RmH194 for growth on succinate verifying that the p*dme-sfcA* construct was functional. pTH513 was introduced into several *S. meliloti* malic enzyme deficient mutants through triparental matings, and transductions were carried out to verify recombination at the *dme* gene locus.

Production of *dme*Δc construct. pTH139 (9) carrying the entire *dme* open reading frame was digested with PstI and religated to remove the C-terminal region of *dme* and leave only the first 449 amino acids of DME. The truncated *dme* gene (*dme*Δc) was removed from the resulting plasmid (pTH452) via digestion with HindIII and XbaI and inserted into pUCP30T digested with the same enzymes to produce pTH458. A triparental mating was carried out to introduce the construct into *dme*::Tn*5* mutant *S. meliloti* strains, and transductions were carried out to verify recombination at the *dme* gene loci as described above.

Enzyme assays and plant tests. For both free-living cells and bacteroid samples, pyruvate formation assays were carried out in the presence of either 1.5 mM NAD^+ or $NADP^+$ to determine DME or TME activity, respectively, as previously described (9). Malate dehydrogenase assays were utilized to verify cell and bacteroid extract integrity (9), with the change in absorption at 340 nm recorded with a Varian Cary 1E UV-visible spectrophotometer for approximately 3 to 5 min. Protein concentrations were determined using the Bio-Rad protein assay.

Plant assays with *Medicago sativa* var. Iroquois were carried out using Leonard assemblies following the method described by Yarosh et al. (42). Triplicate pots of 10 to 12 seedlings were grown, and 28 days postinoculation the plants were harvested. Acetylene reduction assays were carried out with three root systems per pot according to the method of Yarosh et al. (42), and the plants themselves were dried for 3 weeks, after which time the dry weights were recorded.

Native polyacrylamide gel electrophoresis (PAGE) and Western blots. Native polyacrylamide gels (7%) were produced as previously described (26). Portions of 30 μg per sample of crude cell or bacteroid extract were electrophoresed at 4°C with a constant current of 4 mA for 1 h and 7 mA thereafter until the dye front was 1 cm from the end of the gel. Following electrophoresis, the gels were rinsed and stained for NAD^+-dependent malic enzyme activity as previously described (26).

Polyclonal antibodies were obtained by repeated injection of female specific-pathogen-free rabbits with 200 μg of purified DME or TME protein (39). Polyclonal antibodies produced in this way were specific for the respective antigen and reacted with denatured protein. Proteins were transferred from 7% sodium dodecyl sulfate (SDS)-polyacrylamide gels to Immobilon P membranes (Millipore) and treated with anti-TME or anti-DME antibody (a 1/10,000 dilution) for 60 min. The membranes were then exposed to the secondary antibody (anti-rabbit antibody–peroxidase; Sigma) for 30 min and developed using enhanced chemiluminescence reagent (Amersham).

Quantification of the malic enzymes. In order to quantify the DME and TME present in free-living cells and bacteroids, two Western blots for each protein were produced. *S. meliloti* cell extracts were obtained from an overnight LBmc-grown culture, while bacteroids were obtained from alfalfa plants inoculated with wild-type *S. meliloti*. Each SDS-PAGE gel had a constant amount of total free-living protein, with one gel containing various amounts of purified protein while the second had various amounts of total bacteroid protein. Two exposures (30 s and 1 min) were used for each Western blot, and a laser densitometer was used to measure the relative intensities of DME and TME. Two separate standard curves for the purified proteins were produced, and these were used to estimate the amount of DME or TME per 2 μg of free-living-cell extract. The values obtained for TME and DME were then used as a standard to estimate the amount of each protein in bacteroid extracts by comparing the intensity of the 2 μg of total protein from free-living cells to the standard curves of total bacteroid protein.

RESULTS

Quantification of DME and TME levels in bacteroids from alfalfa nodules. Our previous studies suggested that *tme* expression and TME activity were reduced relative to DME in N_2-fixing bacteroids (7, 8). To precisely determine the levels of DME and TME in free-living cells and N_2-fixing bacteroids, we chose to employ antibodies raised against the *S. meliloti* DME and TME proteins which had been overproduced in *E. coli* and purified as previously described (39). These antibodies could be used to directly quantify the two enzymes in crude cell extracts, since the anti-DME antibodies failed to cross-react with TME and the anti-TME antibodies failed to cross-react with DME in Western blots of total cell extracts. Standard curves were produced using purified DME and TME, and these curves were used to estimate the amounts of the two proteins in both free-living cells and bacteroids. The results obtained from the Western blots (see Fig. S1 in the supplemental material) indicate that there is 6.8 ± 0.6 ng of DME/μg of protein from free-living cells and 4.7 ± 0.6 ng of TME/μg of protein from free-living cells. Bacteroids contained 14.2 ± 0.6 ng of DME/μg of total protein and 0.9 ± 0.003 ng of TME/μg of total protein. Hence, TME protein levels in bacteroids are reduced to 20% of the TME levels in free-living cells and are also reduced to 6% relative to the level of DME protein in bacteroids. The reduction in TME protein levels detected in bacteroids versus free-living cells verified the previous activity studies (8), and a reexamination of the activity data for free-living cells and bacteroids (e.g., see Table 3 in reference 7 and Table 4 in reference 8) revealed that in all cases the DME activity levels in bacteroids were approximately 40% higher than those in free-living cells.

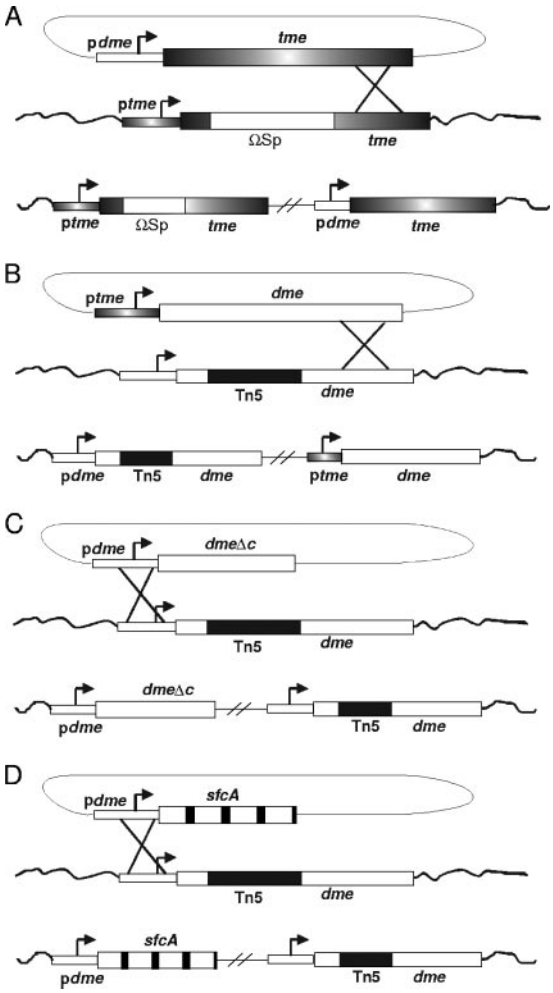

FIG. 1. Schematic outlining the integration of the various *tme* and *dme* constructs into the *S. meliloti* genome. A. Integration of the p*tme-dme* plasmid pTH597 into the *tme*::ΩSp locus. B. Integration of the p*dme-tme* plasmid pTH433 at the *dme*::Tn*5* locus. C. Integration of the *dme*Δ*c* plasmid pTH458 at the *dme*::Tn*5* locus. D. Integration of the p*dme-sfcA* plasmid pTH513 at the *dme*::Tn*5* locus.

TME cannot replace the need for DME in symbiotic N_2 fixation. In a previous study, it was shown that increasing the TME activity in free-living cells overcame the *dme*-dependent succinate growth-negative phenotype of *S. meliloti* strain RmG443 (*pckA pod1 dme-2*::Tn*5*) (8). We therefore wished to determine whether increasing the level of TME activity in bacteroids would allow *dme* mutant strains to fix N_2 in nodules. To accomplish this, we placed the *tme* structural gene under the control of the *dme* promoter, as this should ensure appropriate *tme* expression and appropriate TME activity in N_2-fixing bacteroids. Since the transcriptional start site for both the *tme* and *dme* genes had been determined and since the translational start sites for both genes have been confirmed through the N-terminal sequence of purified DME and TME proteins (26, 39), we were able to interchange the malic enzyme promoters and the structural genes with minimal ambiguity. Oligonucleotide-directed mutagenesis was employed to introduce an SphI site at the ATG start codon for each gene, and the *dme* promoter region was then cloned upstream of the

TABLE 1. *S. meliloti* strains expressing *tme* from the *dme* promoter

Strain	Genotype	Activity in free-living cells			ARA[c]	Plant dry wt (mg)[d]	Activity in bacteroids		
		NAD^+ dependent[a]	$NADP^+$ dependent[a]	MDH[b]			NAD^+ dependent[a]	$NADP^+$ dependent[a]	MDH[b]
Rm1021	Wild type	58 ± 4	74 ± 6	739 ± 15	1,221 ± 320	50.5 ± 0.8	45 ± 1	19 ± 1	2,608 ± 59
RmG455	Rm1021 *dme-3*::Tn*5*	21 ± 2	61 ± 2	611 ± 9	7 ± 3	10 ± 1	ND	ND	2,512 ± 190
RmG994	Rm1021 *dme-3*::Tn*5* *tme-4*::ΩSp	21 ± 1	ND[e]	864 ± 25	ND	10.6 ± 1	ND	ND	3,769 ± 136
RmG995	Rm1021 *tme-4*::ΩSp	72 ± 5	ND	782 ± 19	1,156 ± 258	53.1 ± 2.8	50 ± 2	8 ± 1	3,269 ± 85
RmH897	RmG994::p*dme-tme*	24 ± 1	104 ± 8	684 ± 12	24 ± 6	11.3 ± 0.4	ND[g]	89 ± 2[g]	2,864 ± 63
RmH898	RmG995::p*dme-tme*	70 ± 3	134 ± 5	704 ± 11	563 ± 176	44.8 ± 2.6	52 ± 3	60 ± 1	3,299 ± 72
RmH899	RmG994::p*dme-tme*	14 ± 1	67 ± 5	695 ± 16	15 ± 5	12.3 ± 0.9	—[f]	—	—
RmH900	RmG995::p*dme-tme*	47 ± 1	86 ± 5	1,062 ± 11	—	—	—	—	—
None (uninoculated)	—	—	—	—	—	8.5 ± 0.4	—	—	—

[a] Specific activity, expressed as nanomoles of pyruvate formed/minute/mg protein. Values are means ± standard errors for triplicate samples.
[b] Malate dehydrogenase (MDH) specific activity, expressed as nanomoles NADH formed/minute/mg protein. Values are means ± standard errors for triplicate samples.
[c] ARA, acetylene reduction activity, expressed as nanomoles of ethylene produced per minute per plant and presented as means for triplicate samples containing three root systems each ± standard errors.
[d] Means for triplicate pots containing 7 to 10 plants each ± standard errors.
[e] ND, none detected.
[f] —, not applicable or not tested.
[g] Samples were incubated for 30 min at 30°C.

tme structural gene ATG codon. The *dme* promoter with the *tme* structural gene is referred to as p*dme-tme*, and this construct, in the plasmid pTH433, was inserted into the *S. meliloti dme* mutant genome via a single crossover recombination as outlined in Fig. 1A (see Materials and Methods).

All strains in which the *tme* gene was expressed from the *dme* promoter (RmH897 and RmH898) showed elevated levels of $NADP^+$-dependent malic enzyme in extracts from free-living cells relative to the parental wild-type and RmG455 *dme* mutant *S. meliloti* strains (Table 1). The symbiotic phenotypes of the various strains were determined by measuring the dry weights and acetylene-reducing (nitrogenase) activities of plants some 30 days after inoculation of alfalfa seedlings with these strains. Plants inoculated with *dme* strains expressing *tme* from the *dme* promoter (RmH897 and RmH899) had only residual acetylene reduction activity comparable to that of the plants inoculated with their *dme*-deficient parent *S. meliloti* strains (RmG455 and RmG994) (Table 1). Strain RmH898 that expressed the p*dme-tme* construct in a dme^+ background had reduced acetylene reduction activity; however, this is likely due to experimental variation, since these plants had only marginally reduced average plant dry weights relative to plants inoculated with Rm1021. For other strains, the average plant dry weight determinations mirrored the acetylene reduction data.

Enzyme assays carried out on extracts of bacteroids isolated from the nodules revealed elevated levels of $NADP^+$-dependent activity in strains expressing *tme* from the *dme* promoter (RmH897 and RmH898) compared to Rm1021 bacteroids (Table 1). Similarly, analysis using TME-specific antibodies revealed elevated TME levels in all strains expressing *tme* from the *dme* promoter (RmH897, RmH898, RmH899, and RmH900) (Fig. 2, lanes 6 to 9), whereas no TME was detected in the *tme* mutant RmG994 (Fig. 2, lanes 2 and 5). As described above, the levels of TME in the Rm1021 and RmG455 (*dme3*::Tn*5*) bacteroids were very low (Fig. 2, lanes 3 and 4). The duplication of the *dme* promoter region that occurred in p*dme-tme* cointegrate strains did not appear to effect *dme* expression, as levels of DME protein, as detected with antibodies (data not shown), and DME enzyme activity levels in these strains (RmH897 to RmH900) were comparable to those in the wild type (Table 1). In summary, together these data demonstrated that TME could not function in place of DME for N_2 fixation in bacteroids.

Reduced DME synthesis reduces symbiotic N_2 fixation in *S. meliloti*. The results from experiments in which *tme* expression was increased in bacteroids raised the question of how much DME activity is required for N_2 fixation. Accordingly, we constructed strains in which the *dme* gene was under- and overexpressed. To reduce *dme* expression, the *dme* promoter region upstream from the *dme* ATG start codon was replaced by the symbiotically weak *tme* promoter. The resulting p*tme-dme* construct in the plasmid pTH597 was recombined via a single crossover at the *dme* locus in *dme*, *tme*, and *dme tme* mutant strains as outlined in Fig. 1B (also see Materials and Methods).

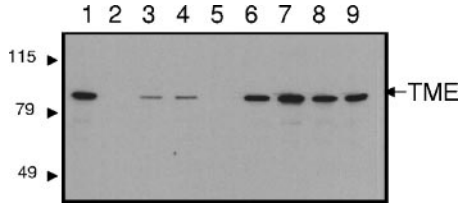

FIG. 2. Western blot to detect TME protein present in *S. meliloti* extracts. Total bacteroid protein was loaded at 2 μg per sample, while 2 μg of free-living-cell extract from *S. meliloti* wild-type strain Rm1021 was run as a control. Lane 1, Rm1021 (wild-type free-living-cell extract); lane 2, RmG994 (Rm1021 *dme-3*::Tn*5* *tme-4*::ΩSp); lane 3, Rm1021 (wild-type bacteroid extract); lane 4, RmG455 (Rm1021 *dme-3*::Tn*5*); lane 5, RmG994 (Rm1021, *dme-3*::Tn*5* *tme-4*::ΩSp); lane 6, RmH897 (RmG994::p*dme-tme*); lane 7, RmH898 (RmG995::p*dme-tme*); lane 8, RmH899 (RmG994::p*dme-tme*); lane 9, RmH900 (RmG995::p*dme-tme*). Numbers on the left indicate molecular weight markers.

TABLE 2. Phenotypes of *S. meliloti* strains expressing *dme* from the *tme* promoter

Strain	Genotype	Activity in free-living cells			ARA[c]	Plant dry wt (mg)[d]	Activity in bacteroids		
		NAD^+ dependent[a]	$NADP^+$ dependent[a]	MDH[b]			NAD^+ dependent[a]	$NADP^+$ dependent[a]	MDH[b]
Rm1021	Wild type	107 ± 4	47 ± 2	313.3 ± 3.9	1,004 ± 2	46.8 ± 4.8	115 ± 2	34 ± 3	1,135 ± 13
RmG454	Rm1021, *dme-2*::Tn*5*	52.1 ± 2	60 ± 1	543.1 ± 25.5	13 ± 2	10.1 ± 0.8	14 ± 1	0.9 ± 0.1	62 ± 1
RmG994	Rm1021, *dme-3*::Tn*5* *tme-4*::ΩSp	54 ± 1	5 ± 1	439.3 ± 40.6	ND[e]	9.5 ± 0.5	ND	ND	461 ± 1
RmG995	Rm1021, *tme-4*::ΩSp	114 ± 1	25 ± 2	381 ± 21.5	1,039 ± 69	54.6 ± 8.3	141 ± 2	61 ± 1	672 ± 23
RmH979	RmG454::p*tme-dme*	77 ± 2	65 ± 3	375 ± 26.2	341 ± 73	16.6 ± 1.0	31 ± 1	7 ± 1	317 ± 2
RmH980	RmG994::p*tme-dme*	82 ± 3	4 ± 1	352.5 ± 15	214 ± 34	16.5 ± 1.6	40 ± 1	0.2 ± 0.1	235 ± 7
RmH981	RmG995::p*tme-dme*	124 ± 1	29 ± 5	387.9 ± 24.4	400 ± 106	46.4 ± 6.8	116 ± 2	42 ± 1	155 ± 3
None (uninoculated)	—[f]	—	—	—	—	8.5 ± 1.5	—	—	—

[a] Specific activity, expressed as nanomoles of pyruvate formed/minute/mg protein. Values are means ± standard errors for triplicate samples.
[b] Malate dehydrogenase (MDH) specific activity, expressed as nanomoles NADH formed/minute/mg protein. Values are means ± standard errors for triplicate samples.
[c] ARA, acetylene reduction activity, expressed as nmoles of ethylene produced per minute per plant and presented as means for triplicate samples containing three root systems each ± standard errors.
[d] Means for triplicate pots containing 7 to 10 plants each ± standard error.
[e] ND, none detected.
[f] —, not applicable or not tested.

The symbiotic N_2-fixing abilities and the enzyme activities in both free-living and bacteroid forms of the resulting strains are shown in Table 2. The amounts of DME protein in Western blots of bacteroid extracts as detected with anti-DME antibodies were also determined (Fig. 3). As expected, plants inoculated with *dme* mutant strains (RmG454 and RmG994) failed to fix N_2, as demonstrated by their negligible acetylene reduction (nitrogenase) activity and dry weight values, which were similar to those of uninoculated plants. In contrast, plants inoculated with *dme* mutant strains that also expressed *dme* from the *tme* promoter (RmH979 and RmH980) had 20 to 30% of the acetylene reduction (nitrogenase) activity and 35% of the dry weight of plants inoculated with wild-type Rm1021 (Table 2). These plants were shorter than those inoculated with the wild-type strain but much larger and greener than the uninoculated controls or plants inoculated with the *dme* mutant strains. Thus, expression of *dme* from the *tme* promoter resulted in a sharp reduction in N_2 fixation activity in root nodules.

The enzyme activity measurements demonstrated that while the *tme* promoter was as strong as the *dme* promoter in free-living cells, *dme* expression in bacteroids from this promoter was reduced, as the NAD^+-dependent malic enzyme activity in RmH979 and RmH980 bacteroid extracts was less than 30% of wild-type levels (Table 2). Similarly, the amount of DME protein in the RmH979 and RmH980 bacteroid extracts was clearly smaller than in strains carrying the wild-type *dme* locus (Fig. 3, lanes 1 and 5). We note that despite the absence of DME protein in extracts from *dme* mutant strains (Fig. 3, lane 6), a high residual NAD^+-dependent malic enzyme activity was detected in the crude extracts from free-living cells and bacteroids of *dme* strains (Table 2). This background was also observed previously and is due to cross-reacting activities, including that from malate dehydrogenase, which is present at high levels in these extracts.

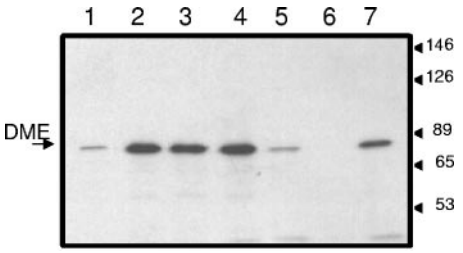

FIG. 3. Western blot to detect DME in bacteroid extracts. Total bacteroid protein was loaded at 2 μg per sample, while 2 μg of free-living-cell extract from *S. meliloti* wild-type strain Rm1021 was run as a control. Numbers on the right indicate molecular weight markers. Lane 1, RmH979 (RmG454::p*tme-dme*); lane 2, RmH981 (RmG995::p*tme-dme*); lane 3, RmG995 (Rm1021 *tme-4*::ΩSp); lane 4, Rm1021 bacteroid extract (wild type); lane 5, RmH980 (RmG994::p*tme-dme*); lane 6, RmG994 (Rm1021 *dme-3*::Tn*5* *tme-4*::ΩSp); lane 7, Rm1021 free-living-cell extract (wild type).

To increase the level of DME in bacteroids, the *dme* locus was cloned into the high-copy-number plasmid pBBR5 (20). NAD^+-dependent malic enzyme activities in bacteroids from Rm1021 carrying this plasmid were 657 nmol/min/mg protein. However, the dry weights of plants inoculated with this strain were not statistically different from those of plants inoculated with wild-type Rm1021, and we therefore conclude that the level of DME in the wild-type bacteroids is not limiting for N_2 fixation. On the other hand, the data from strains in which *dme* was expressed from the *tme* promoter show clearly that reducing the level of DME in bacteroids renders the conversion of malate to pyruvate a rate-limiting reaction for N_2 fixation. Limiting the rate of pyruvate synthesis is likely to limit the flux of malate through the TCA cycle and hence the generation of ATP and perhaps reductant for nitrogenase. It is also possible that reduced levels of pyruvate could limit alanine dehydrogenase-catalyzed alanine synthesis, and that in turn may reduce N_2 fixation (1, 40).

Expression of the 3′-truncated *dme* gene (*dme*Δc) in *S. meliloti dme* mutant strains. The interpretation of the experimental results obtained from manipulations of the TME and DME proteins were complicated by the unusual structure of these proteins. This prompted us to investigate whether the C-terminal PTA-like domain of DME is required for N_2 fixation, since DME deletions that lack this region maintain malic en-

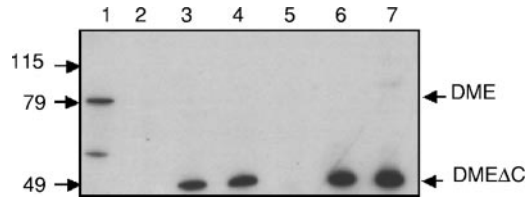

FIG. 4. Western blot to detect DME and DMEΔC proteins in bacteroid extracts. Total bacteroid protein was loaded at 2 μg per sample. Lane 1, Rm1021 (wild type); lane 2, RmG454 (Rm1021 *dme-2*::Tn*5*); lane 3, RmH996 (RmG454::*dme*Δc); lane 4, RmH998 (RmG454::*dme*Δc); lane 5, RmG456 (Rm1021 *dme-1*::Tn*5*); lane 6, RmH999 (RmG456::*dme*Δc); lane 7, RmH1000 (RmG456::*dme*Δc). Numbers on the left indicate molecular weight markers.

zyme activity (26). Accordingly, we constructed a *dme* 3′-deletion derivative, referred to as *dme*Δc, which expressed a truncated DME protein lacking the C-terminal 321 amino acids (DMEΔC). The pTH458 plasmid carrying the *dme*Δc gene and *dme* promoter was recombined via a single crossover into *dme* mutant strains as illustrated in Fig. 1C and described in Materials and Methods.

The symbiotic phenotypes of these strains were assessed as described above (Tables 1 and 2). Plants inoculated with *dme-1* and *dme-2* strains carrying *dme*Δc were Fix^+ and had dry weights of 36.4 ± 2.6 mg and 48.3 ± 0.1 mg, respectively, compared to 40.6 ± 3.7 mg for plants inoculated with the wild type strain Rm1021 and 7.1 ± 1.0 mg and 7.4 ± 0.6 mg for plants inoculated with the *dme* mutant strains. Enzyme assays of bacteroid extracts from *dme* strains carrying *dme*Δc had NAD^+-dependent malic enzyme activity that was comparable to wild-type levels of 71 nmol/min/mg protein. Western blots of these bacteroid extracts showed that strains expressing *dme*Δc produced only the truncated malic enzyme migrating at 49 kDa, compared to the 82 kDa full-length DME protein (Fig. 4). These data verified that the symbiotic phenotype observed was due to the expression of the truncated gene, *dme*Δc, and not to regeneration of an intact *dme* gene. These results established that the PTA-like C-terminal domain of DME is not required for N_2 fixation, and this prompted us to investigate whether a heterologous NAD^+ malic enzyme such as that from *Escherichia coli* could replace the function of DME in N_2-fixing bacteroids.

The *Escherichia coli* NAD^+-dependent malic enzyme ScfA can replace DME in N_2-fixing bacteroids. The *E. coli* $NAD(P)^+$malic enzyme encoded by *sfcA* has only limited homology to other prokaryotic malic enzymes and instead appears to be more closely related to eukaryotic malic enzymes and the *Bacillus subtilis* malic enzyme Mao2.bs (2, 26). The *sfcA* gene encodes a polypeptide of 574 amino acids and lacks the PTA-like C-terminal region present in DME and TME. An alignment of the *scfA*-encoded protein with the N-terminal malic enzyme region of DME revealed that while the two proteins share only 25% identity, the conserved regions common to all malic enzymes are identifiable (see Fig. S2 in the supplemental material) (26). To express the *scfA* gene in *S. meliloti*, *scfA* was cloned downstream of the *dme* promoter to give a p*dme-scfA* construct in the plasmid pTH513. The *E. coli* NAD^+-dependent malic enzyme could clearly function in *S. meliloti* free-living cells, since cointegration of the p*dme-sfcA* plasmid, pTH513, in RmH194 (*pckA1*::Tn*3*HoHo *pod-1 dme-1*::Tn*5 tme-4*::ΩSp) restored the ability of this strain to grow on succinate. To investigate whether *sfcA* could function symbiotically in root nodules, the pTH513 plasmid was recombined at the *dme* locus in various *dme*, *dme tme*, and *tme* mutant strains. The symbiotic phenotype of these strains revealed that the *E. coli* NAD^+-dependent malic enzyme restored near-wild-type activity to the *dme* mutant strains, with plant dry weights varying from 65 to 84% of that of the wild-type-inoculated plants (RmK215, RmK216, RmK217, and Rm1021) (Table 3). Student's *t* test showed no statistical significant difference between dry weight values for the wild-type-inoculated and the RmK215-, RmK216-, and RmK217-inoculated plants. Enzyme assays conducted with *dme* mutant bacteroids expressing *sfcA* revealed approximately half (44 to 59%) of the NAD^+-dependent malic enzyme activity present in wild-type bacteroids (Table 3). Native PAGE gels stained

TABLE 3. Phenotypes of *S. meliloti* strains expressing the *sfcA* gene under the control of the *dme* promoter

Strain	Genotype	Activity in free-living cells		Plant dry wt (mg)[c]	Activity in bacteroids	
		NAD^+ dependent[a]	MDH[b]		NAD^+ dependent[a]	MDH[b]
Rm1021	Wild type	64 ± 1	543 ± 11	40.6 ± 3.7	103 ± 2	3,172 ± 68
RmG455	Rm1021 *dme-3*::Tn*5*	26 ± 15	713 ± 20	7.4 ± 0.6	8 ± 1	3,401 ± 94
RmG456	Rm1021 *dme-1*::Tn*5*	29 ± 9	717 ± 16	7.1 ± 1.0	8 ± 2	3,103 ± 60
RmG994	Rm1021 *dme-3*::Tn*5 tme-4*::ΩSp	30 ± 4	725 ± 37	8.8 ± 0.6	ND[d]	2,251 ± 72
RmG995	Rm1021 *tme-4*::ΩSp	67 ± 3	583 ± 14	45.9 ± 4.1	94 ± 3	3,198 ± 139
RmK215	RmG455::p*dme-sfcA*	122 ± 20	713 ± 44	34.3 ± 3.2	50 ± 1	2,909 ± 47
RmK216	RmG456::p*dme-sfcA*	99 ± 10	598 ± 4	33.9 ± 6.6	46 ± 1	4,073 ± 214
RmK217	RmG994::p*dme-sfcA*	85 ± 13	589 ± 22	26.3 ± 1.4	61 ± 1	2,739 ± 300
RmK218	RmG995::p*dme-sfcA*	135 ± 12	722 ± 37	50.6 ± 3.5	77 ± 11	2,925 ± 55
RmK219	Rm1021::p*dme-sfcA*	114 ± 11	612 ± 17	59.4 ± 11.2	74 ± 1	2,894 ± 28
None (uninoculated)	—[e]	—	—	6.3 ± 0.4	—	—

[a] Specific activity, expressed as nanomoles of pyruvate formed/minute/mg protein. Values are means for triplicate samples ± standard errors.
[b] Malate dehydrogenase (MDH) specific activity, expressed as nanomoles NADH formed/minute/mg protein. Values are means for triplicate samples ± standard errors.
[c] Expressed as means for triplicate pots containing 7 to 10 plants each ± standard errors.
[d] ND, none detected.
[e] —, not applicable or not tested.

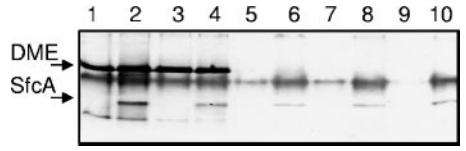

FIG. 5. Nondenaturing PAGE to show NAD^+-dependent malic enzyme in bacteroid extracts of *S. meliloti* expressing *sfcA*. Protein was loaded at 30 μg per sample, and the gel was stained to detect NAD^+-dependent malic enzyme activity. Lane 1, Rm1021 (wild type); lane 2, RmK219 (Rm1021::p*dme-sfcA*); lane 3, RmG995 (Rm1021 *tme-4*::ΩSp); lane 4, RmK218 (RmG995::p*dme-sfcA*); lane 5, RmG455 (Rm1021 *dme-3*::Tn*5*); lane 6, RmK215 (RmG455::p*dme-sfcA*); lane 7, RmG456 (Rm1021 *dme-1*::Tn*5*); lane 8, RmK216 (RmG456::p*dme-sfcA*); lane 9, RmG994 (Rm1021 *dme-3*::Tn*5* *tme-4*::ΩSp); lane 10, RmK217 (RmG994::p*dme-sfcA*).

for NAD^+-dependent malic enzyme activity revealed that the *scfA*-encoded protein was present in the RmK215, RmK216, and RmK217 bacteroid extracts and that, as expected, no DME was present (Fig. 5.) These data demonstrate that the *E. coli* NAD^+-dependent malic enzyme is capable of restoring wild-type N_2-fixing activity to *S. meliloti dme* mutant strains and confirm that the DME C-terminal PTA-like domain is not required for N_2 fixation.

DISCUSSION

Why NAD^+-dependent malic enzyme (DME) is required for symbiotic N_2 in alfalfa root nodules remains to be unambiguously established. We have previously suggested that the DME-NAD^+ malic enzyme together with pyruvate dehydrogenase convert malate to acetyl-CoA and that this is an essential anaplerotic pathway for cells metabolizing C_4-dicarboxylic acids via the TCA cycle (7, 26). However, it is also possible that DME is required to generate pyruvate as a precursor for some other important metabolic pathways in bacteroids. Pyruvate could be a precursor in the yet-to-be-defined pathway leading to the generation of reductant for nitrogenase (35). Another possible pathway could be alanine synthesis in nodules. However, this is unlikely, given that alanine dehydrogenase mutants of *R. leguminosarum* and *M. loti* form Fix^+ nodules (21, 24). The finding that reduced NAD^+ malic enzyme synthesis reduces N_2 fixation suggests that a minimal malate-to-pyruvate flux is required in alfalfa bacteroids to maintain efficient N_2 fixation. Our biochemical characterization of the DME and TME proteins and all of the physiological evidence suggest that these enzymes function solely in the synthesis of pyruvate from malate (9, 39).

The observation that low levels of NAD^+ malic enzyme in bacteroids supported significant symbiotic N_2 fixation is in contrast to the finding that increasing the levels of $NADP^+$ malic enzyme in bacteroids failed to support detectable N_2-fixing activity in *dme* mutants. This result is more striking given that the $NADP^+$ malic enzyme can function in place of DME in allowing a *S. meliloti pckA1 pod-1 dme-1*::Tn*5* *tme-4*::ΩSp mutant to grow on succinate as a carbon source. The ability of the C-terminal-deletion derivative of DME together with the ability of the *E. coli* NAD^+ malic enzyme to restore wild-type N_2-fixing activity to *S. meliloti dme* mutants clearly demonstrates that the PTA-like domain of DME is not required for N_2 fixation. Moreover, this strongly suggests that the failure of TME to replace DME in N_2-fixing bacteroids is unrelated to differences in their PTA-like C-terminal domains.

DME has K_ms of 9.4 mM for L-malate and 89 μM for NAD^+, while TME has K_ms for malate and $NADP^+$ of 12.5 mM and 33 μM, respectively (39). The TME V_{max} of 53 μmol/min/mg protein is close to the DME V_{max} of 60 μmol/min/mg protein. Overall, the kinetic parameters for DME and TME are similar, and therefore it appears unlikely that these account for the different symbiotic properties of the two enzymes. However, unlike the $NADP^+$-dependent malic enzyme, the *S. meliloti* NAD^+ malic enzyme is allosterically regulated, with acetyl-CoA inhibiting and succinate and fumarate activating activity (39). Since kinetic results in our laboratory have revealed that DMEΔC is no longer allosterically regulated (unpublished results), and since DMEΔC functions in place of DME in nodules, we can conclude that the allosteric nature of DME is not essential to its function in bacteroids.

The *E. coli* NAD^+ malic enzyme was characterized by several groups, and K_m values for the substrate L-malate have been reported in the range from 0.1 to 0.4 mM, while the K_m for the NAD^+ cofactor has been estimated to be 23 and 55 μM (17, 33, 36, 41). As in the case of DME, the *E. coli* NAD^+ malic enzyme is allosterically regulated, with inhibition of activity by acetyl-CoA and activation by malate (9, 28, 32, 39). Thus, except for a higher affinity for L-malate, the *E. coli* NAD^+ malic enzyme compares favorably with DME, and it is not surprising that the *E. coli* enzyme can function in place of DME. However, as the two enzymes share little amino acid similarity, it would appear that the ability of the *E. coli* enzyme to function in bacteroids simply reflects its ability to catalyze the NAD^+-dependent conversion of malate to pyruvate.

Given that neither differences in the catalytic rate nor the affinity for L-malate is sufficient to account for the failure of TME to act in place of DME in N_2-fixing bacteroids, we hypothesize that there is a high ratio of $NADPH^+ + H^+/NADP^+$ in bacteroids and that this prevents TME from functioning in nodules. The ratios of $NAD(P)H^+ + H^+/NAD(P)^+$ in bacteroids from alfalfa nodules have not been determined; however, the levels in soybean bacteroids have been reported in two studies. Tezuka and Murayama (38) reported NAD/NADH and NADP/NADPH ratios for soybean bacteroids of 5.56 and 3.26, respectively. These values are higher than those reported by Tajima and Kouzai (37), which were 2.17 and 0.37, respectively. Possible reasons for the different results, such as methods used in the extraction and assay of pyridine nucleotides in bacteroids, have been discussed (38). Nevertheless, the very different values for the NADP/NADPH ratios (3.26 and 0.37) do not allow us to draw inferences; interpretations are also complicated by the fact that the properties of the *Bradyrhizobium japonicum* NAD^+ and $NADP^+$ malic enzymes appear to differ from those of the *S. meliloti* DME and TME enzymes, and it has been suggested that the physiological roles of the enzymes are different in *S. meliloti* and *B. japonicum* (4, 5).

The hypothesis that there is a high ratio of $NADPH^+ + H^+$ to $NADP^+$ in bacteroids is difficult to reconcile with the observations that *S. meliloti* isocitrate dehydrogenase (Idh) is an $NADP^+$-dependent enzyme and that mutants deficient for this activity are unable to support symbiotic nitrogen fixation, as determined by McDermott and Kahn (25). Isocitrate dehydro-

genase has been purified from *S. meliloti* and has a K_m of 15 μM for $NADP^+$ (3), which is half that of TME (39). This low K_m may be a reason why isocitrate dehydrogenase is capable of functioning under conditions of restricted $NADP^+$ while TME cannot. Interestingly, an NAD^+-dependent isocitrate dehydrogenase has been reported for rhizobia infecting *Lotus pedunculatus*; however, this does not appear to be a widespread phenomenon among prokaryotes (27). To directly address the issue of cofactor dependence, we wish to alter the cofactor specificity of TME from $NADP^+$ to NAD^+ to determine whether such an enzyme would support N_2 fixation by a *dme* mutant strain.

Microbial genome sequences have revealed the presence of malic enzyme-like proteins, presumably the NAD^+ and $NADP^+$ enzymes, in many bacteria. In *E. coli*, the presence of two enzymes has been known for some time; however, the distinct roles played by these enzymes have not been clearly defined (17, 28, 33, 41). In *Corynebacterium glutamicum* the *malE*-encoded NADP-dependent malic enzyme plays an important role in routing carbon flux between glycolysis and gluconeogenesis (15, 29). Aymerich and colleagues recently identified and characterized four malic enzyme isoforms from *Bacillus subtilis* (6, 23). Disruption of the *ytsJ* gene resulted in a markedly reduced growth on malate despite the presence of the other enzymes. YtsJ is the sole NADP-dependent malic enzyme, and the mutant phenotype showed that it plays a role distinct from those of the other malic enzymes in *B. subtilis*. Paradoxically, while overexpression of the *E. coli* NADP-dependent malic enzyme in *B. subtilis* did not suppress the malate growth phenotype of the *ytsJ* mutant, overexpression of the *E. coli* transdehydrogenase gene (*udhA*) did partially suppress this phenotype. Those authors concluded that YtsJ may play an additional physiological role beyond the conversion of malate to pyruvate. It is clear that much remains to be established regarding the physiological roles of malic enzyme, and accordingly the analysis of the *Sinorhizobium* DME and TME enzymes and the establishment of their roles should be informative with respect to general microbial metabolism.

ACKNOWLEDGMENTS

We express our appreciation to M. Donnely for providing the *sfcA* construct and R. T. Voegele and S. Vlaar for analyzing the biochemical characteristics of DMEΔC. We thank Punita Anjea and Rahat Zaheer for critical reading of the manuscript.

T.M.F. gratefully acknowledges the financial support from the Natural Sciences and Engineering Research Council of Canada.

REFERENCES

1. **Allaway, D., E. M. Lodwig, L. A. Crompton, M. Wood, R. Parsons, T. R. Wheeler, and P. S. Poole.** 2000. Identification of alanine dehydrogenase and its role in mixed secretion of ammonium and alanine by pea bacteroids. Mol. Microbiol. **36:**508–515.
2. **Boles, E., P. Jong-Gubbels, and J. T. Pronk.** 1998. Identification and characterization of MAE1, the *Saccharomyces cerevisiae* structural gene encoding mitochondrial malic enzyme. J. Bacteriol. **180:**2875–2882.
3. **Chandrasekharan Nambiar, P. T., and Y. I. Shethna.** 1976. Purification and properties of an $NADP^+$-specific isocitrate dehydrogenase from Rhizobium meliloti. Antonie Leeuwenhoek **42:**471–482.
4. **Chen, F., Y. Okabe, K. Osano, and S. Tajima.** 1997. Purification and characterization of the NADP-malic enzyme from Bradyrhizobium japonicum A1017. Biosci. Biotechnol. Biochem. **61:**384–386.
5. **Chen, F., Y. Okabe, K. Osano, and S. Tajima.** 1998. Purification and characterization of an NAD-malic enzyme from *Bradyrhizobium japonicum* A1017. Appl. Environ. Microbiol. **64:**4073–4075.
6. **Doan, T., P. Servant, S. Tojo, H. Yamaguchi, G. Lerondel, K. Yoshida, Y. Fujita, and S. Aymerich.** 2003. The Bacillus subtilis ywkA gene encodes a malic enzyme and its transcription is activated by the YufL/YufM two-component system in response to malate. Microbiology **149:**2331–2343.
7. **Driscoll, B. T., and T. M. Finan.** 1993. NAD^+-dependent malic enzyme of Rhizobium meliloti is required for symbiotic nitrogen fixation. Mol. Microbiol. **7:**865–873.
8. **Driscoll, B. T., and T. M. Finan.** 1996. $NADP^+$-dependent malic enzyme of *Rhizobium meliloti*. J. Bacteriol. **178:**2224–2231.
9. **Driscoll, B. T., and T. M. Finan.** 1997. Properties of NAD^+- and $NADP^+$-dependent malic enzymes of Rhizobium (Sinorhizobium) meliloti and differential expression of their genes in nitrogen-fixing bacteroids. Microbiology **143:**489–498.
10. **Finan, T. M., E. Hartweig, K. LeMieux, K. Bergman, G. C. Walker, and E. R. Signer.** 1984. General transduction in *Rhizobium meliloti*. J. Bacteriol. **159:** 120–124.
11. **Finan, T. M., B. Kunkel, G. F. De Vos, and E. R. Signer.** 1986. Second symbiotic megaplasmid in *Rhizobium meliloti* carrying exopolysaccharide and thiamine synthesis genes. J. Bacteriol. **167:**66–72.
12. **Finan, T. M., I. Oresnik, and A. Bottacin.** 1988. Mutants of *Rhizobium meliloti* defective in succinate metabolism. J. Bacteriol. **170:**3396–3403.
13. **Finan, T. M., J. M. Wood, and D. C. Jordan.** 1983. Symbiotic properties of C4-dicarboxylic acid transport mutants of *Rhizobium leguminosarum*. J. Bacteriol. **154:**1403–1413.
14. **Fischer, H. M.** 1994. Genetic regulation of nitrogen fixation in rhizobia. Microbiol. Rev. **58:**352–386.
15. **Gourdon, P., M. F. Baucher, N. D. Lindley, and A. Guyonvarch.** 2000. Cloning of the malic enzyme gene from *Corynebacterium glutamicum* and role of the enzyme in lactate metabolism. Appl. Environ. Microbiol. **66:** 2981–2987.
16. **Hansen, E. J., and E. Juni.** 1975. Isolation of mutants of *Escherichia coli* lacking NAD- and NADP-linked malic. Biochem. Biophys. Res. Commun. **65:**559–566.
17. **Katsuki, H., K. Takeo, K. Kameda, and S. Tanaka.** 1967. Existence of two malic enzymes in Escherichia coli. Biochem. Biophys. Res. Commun. **27:** 331–336.
18. **Kawai, S., H. Suzuki, K. Yamamoto, M. Inui, H. Yukawa, and H. Kumagai.** 1996. Purification and characterization of a malic enzyme from the ruminal bacterium *Streptococcus bovis* ATCC 15352 and cloning and sequencing of its gene. Appl. Environ. Microbiol. **62:**2692–2700.
19. **Kobayashi, K., S. Doi, S. Negoro, I. Urabe, and H. Okada.** 1989. Structure and properties of malic enzyme from Bacillus stearothermophilus. J. Biol. Chem. **264:**3200–3205.
20. **Kovach, M. E., P. H. Elzer, D. S. Hill, G. T. Robertson, M. A. Farris, R. M. Roop, and K. M. Peterson.** 1995. Four new derivatives of the broad-host-range cloning vector pBBR1MCS, carrying different antibiotic-resistance cassettes. Gene **166:**175–176.
21. **Kumar, S., A. Bourdes, and P. Poole.** 2005. De novo alanine synthesis by bacteroids of Mesorhizobium loti is not required for nitrogen transfer in the determinate nodules of *Lotus corniculatus*. J. Bacteriol. **187:**5493–5495.
22. **Kunkel, T. A., J. D. Roberts, and R. A. Zakour.** 1987. Rapid and efficient site-specific mutagenesis without phenotypic selection. Methods Enzymol. **154:**367–382.
23. **Lerondel, G., T. Doan, N. Zamboni, U. Sauer, and S. Aymerich.** 2006. YtsJ has the major physiological role of the four paralogous malic enzyme isoforms in *Bacillus subtilis*. J. Bacteriol. **188:**4727–4736.
24. **Lodwig, E., S. Kumar, D. Allaway, A. Bourdes, J. Prell, U. Priefer, and P. Poole.** 2004. Regulation of L-alanine dehydrogenase in *Rhizobium leguminosarum* bv. viciae and its role in pea nodules. J. Bacteriol. **186:**842–849.
25. **McDermott, T. R., and M. L. Kahn.** 1992. Cloning and mutagenesis of the *Rhizobium meliloti* isocitrate dehydrogenase gene. J. Bacteriol. **174:**4790–4797.
26. **Mitsch, M. J., R. T. Voegele, A. Cowie, M. Osteras, and T. M. Finan.** 1998. Chimeric structure of the NAD(P)+- and NADP+-dependent malic enzymes of Rhizobium (Sinorhizobium) meliloti. J. Biol. Chem. **273:**9330–9336.
27. **Moustafa, E., and C. K. Leong.** 1975. Effect of adenine nucleotides on NAD-dependent isocitrate dehydrogenases in rhizobia and bacteroids of legume root nodules. Biochim. Biophys. Acta **391:**9–14.
28. **Murai, T., M. Tokushige, J. Nagai, and H. Katsuki.** 1971. Physiological functions of NAD- and NADP-linked malic enzymes in Escherichia coli. Biochem. Biophys. Res. Commun. **43:**875–881.
29. **Netzer, R., M. Krause, D. Rittmann, P. G. Peters-Wendisch, L. Eggeling, V. F. Wendisch, and H. Sahm.** 2004. Roles of pyruvate kinase and malic enzyme in Corynebacterium glutamicum for growth on carbon sources requiring gluconeogenesis. Arch. Microbiol. **182:**354–363.
30. **Poole, P., and D. Allaway.** 2000. Carbon and nitrogen metabolism in Rhizobium. Adv. Microb. Physiol. **43:**117–163.
31. **Ronson, C. W., P. Lyttleton, and J. G. Robertson.** 1981. C(4)-dicarboxylate transport mutants of Rhizobium trifolii form ineffective nodules on Trifolium repens. Proc. Natl. Acad. Sci. USA **78:**4284–4288.
32. **Sanwal, B. D.** 1970. Allosteric controls of amphibolic pathways in bacteria. Bacteriol. Rev. **34:**20–39.

33. **Sanwal, B. D.** 1970. Regulatory characteristics of the diphosphopyridine nucleotide-specific malic enzyme of Escherichia coli. J. Biol. Chem. **245:** 1212–1216.
34. **Schweizer, H. P.** 2001. Vectors to express foreign genes and techniques to monitor gene expression in Pseudomonads. Curr. Opin. Biotechnol. **12:**439–445.
35. **Scott, J. D., and R. A. Ludwig.** 2004. Azorhizobium caulinodans electron-transferring flavoprotein N electrochemically couples pyruvate dehydrogenase complex activity to N_2 fixation. Microbiology **150:**117–126.
36. **Stols, L., and M. I. Donnelly.** 1997. Production of succinic acid through overexpression of NAD^+-dependent malic enzyme in an *Escherichia coli* mutant. Appl. Environ. Microbiol. **63:**2695–2701.
37. **Tajima, S., and K. Kouzai.** 1989. Nucleotide pools in soybean nodule tissue, a survey of NAD(P)/NAD(P)H ratios and energy charge. Plant Cell Physiol. **30:**589–593.
38. **Tezuka, T., and Y. Murayama.** 2002. Formation of pyridine nucleotides under symbiotic and non-symbiotic conditions between soybean nodules and free-living rhizobia. Phytochemistry **61:**637–644.
39. **Voegele, R. T., M. J. Mitsch, and T. M. Finan.** 1999. Characterization of two members of a novel malic enzyme class. Biochim. Biophys. Acta **1432:**275–285.
40. **Waters, J. K., B. L. Hughes, L. C. Purcell, K. O. Gerhardt, T. P. Mawhinney, and D. W. Emerich.** 1998. Alanine, not ammonia, is excreted from N_2-fixing soybean nodule bacteroids. Proc. Natl. Acad. Sci. USA **95:** 12038–12042.
41. **Yamaguchi, M., M. Tokushige, and H. Katsuki.** 1973. Studies on regulatory functions of malic enzymes. II. Purification and molecular properties of nicotinamide adenine dinucleotide-linked malic enzyme from Escherichia coli. J. Biochem. (Tokyo) **73:**169–180.
42. **Yarosh, O. K., T. C. Charles, and T. M. Finan.** 1989. Analysis of C4-dicarboxylate transport genes in Rhizobium meliloti. Mol. Microbiol. **3:**813–823.
43. **Yurgel, S. N., and M. L. Kahn.** 2004. Dicarboxylate transport by rhizobia. FEMS Microbiol. Rev. **28:**489–501.